EUROPEAN ORGANIZATION FOR NUCLEAR RESEARCH

Proposal to the ISOLDE and Neutron Time-of-Flight Committee

# Effects of the neutron halo in $^{15}$C scattering at energies around the Coulomb barrier

31-May-2016

I. Martel[1,2], X. Aslanoglou[3] , L. A. Acosta[4], L. Barrón-Palos[4], MJG. Borge[1,5], T. Cap[6], E. Chávez-Lomelí[4], A. Di Pietro[6], P. Figuera[6], JP. Fernández[6], A. Huerta-Hernandez[4], N. Keeley[7], R. Kotak[8], R. Lica[1], M. Madurga[1], G. Marquínez-Durán[2], A. Pakou[3], K. Rusek[9], A.K. Orduz[2], R. Raabe[10], N. Soic[11], O. Sgouros[3], A.M. Sánchez-Benítez[2], V. Soukeras[3], O. Tengblad[5], A. Trzcinska[7], M.Wolinska-Cichocka[7], R. Wolski[12]

[1] PH Department, CERN, CH-1211 Geneva 23, Switzerland.
[2] University of Huelva, Avda Fuerzas Armadas sn, 21971 Huelva, Spain.
[3] Department of Physics and HINP, The University of Ioannina, Ioannina, Greece.
[4] Departamento de Física Experimental del Instituto de Física, Universidad Nacional Autónoma de México. Aptdo 20-364, México D. F. 01000, Mexico.
[5] Instituto de Estructura de La Materia – CSIC. Serrano 113 bis, ES-28006 Madrid, Spain.
[6] INFN - Laboratori Nazionali del Sud, via S.Sofia 62, 95123 Catania, Italy.
[7] Srodowiskowe Laboratorium Ciężkich Jonów, Uniwersytet Warszawski, Pasteura 5A, 02-093 Warszawa, Poland.
[8] Astrophysics Research Centre, School of Mathematics and Physics, Queen's University Belfast, Belfast, County Antrim, BT7 1NN, United Kingdom.
[9] National Centre for Nuclear Research, ul. Andrzeja Sołtana 7, 05-400 Otwock, Poland.
[10] Instituut voor Kern- en Stralingsfysica, Celestijnenlaan 200d - bus 2418, B-3001 Heverlee, Belgium.
[11] Rudjer Boskovic Institute, Bijenicka cesta 54, HR-10000 Zagreb, Croatia.
[12] Henryk Niewodniczanski Institute of Nuclear Physics PAS, Cracow.

Spokesperson(s): I. Martel (ismael.martel.bravo@cern.ch), O. Tengblad (olof.tengblad@cern.ch)

Local contact: Razvan Lica (Razvan.Lica@cern.ch)



## Abstract

We propose to study the low energy dynamics of the halo nucleus $^{15}$C ($S_n$ = 1215 keV) by measuring the angular distribution of the elastic scattering and $^{14}$C production cross sections at Coulomb barrier energies. The carbon isotope $^{15}$C is a rather unique nucleus as its ground state exhibits the only known pure s-wave halo configuration. The halo structure favours breakup and neutron stripping to bound states, and these effects should be observable as a sudden decrease in the angular distribution of the elastic channel around the grazing angle. This would be the first dynamical study carried out so far for the halo nucleus $^{15}$C at low collision energies, which should bring information on the complicated coupling between elastic, neutron transfer and breakup channels, and the role of the continuum.

**Requested shifts:** [30] shifts
**Beamline:** 2nd beamline HIE-Isolde

## 1 INTRODUCTION

Nuclear systems, such as $^{6}$He, $^{11}$Li, $^{11}$Be, $^{14}$B, $^{15,19,22}$C or $^{31}$Ne, are known to have an extended neutron distribution, the so-called neutron halo [1]. The halo can be formed when the separation energy of valence neutrons is much smaller than the average binding energy per nucleon, so that they can tunnel out the nuclear potential up to large distances with sizeable probability. This effect enhances the diffuseness of the nuclear surface, leading to a "delocalization" of the wave function and to an extended density distribution. Therefore the nuclear system can be pictured as a "halo" structure surrounding the small, tightly bound, nuclear core.

During last decades there has been an intense experimental and theoretical activity dedicated to study the appearance of haloes, the structure of these states, and the dynamics of the system in reaction processes. Quasi-free nucleon-knockout reactions at high energies (E ~ 100 MeV/u) have been widely used to extract relevant properties of these exotic structures. The halo produces a pronounced maxima in the Coulomb dipole strength B(E1) just above the neutron separation energy, very narrow transverse momentum distributions and large interaction cross-sections [2].

At lower energies (E~ 5 MeV/u), just around the Coulomb barrier, the dynamics of the reaction is dominated by the coupling between the elastic channel and collective excitations, neutron transfer and breakup. The angular distributions of the elastic cross sections and the core fragments present large sensitivity to these couplings effects, which are due to the halo structure. This has been demonstrated in previous studies carried out by our collaboration with lighter exotic beams of $^{11}$Be, $^{11}$Li and $^{6}$He [3 -10] scattered from heavy targets. For these nuclei the angular distribution of the elastic channel shows a strong absorption pattern where the Coulomb rainbow, a typical feature of non-halo nuclei at near-barrier energies, completely disappears. The angular distributions of breakup and transfer are largely produced by dipole couplings to the continuum, and present very high yields even at deep Sub-Coulomb barrier energies. In light halo systems it is also found that elastic and reaction cross sections follow a systematic behaviour with angle and energy, respectively, suggesting a decoupling between core and halo degrees of freedom during the reaction process [11, 12]. To understand the role of the halo in low energy collisions it is interesting to extend these studies to heavier systems like the case of $^{15}$C. In addition, the presence of an extended neutron distribution will also affect low energy capture reactions relevant for astrophysics and some studies have been performed in the past [2, 13, 14].

The experiments performed in the past with stable beams have shown that the Optical Model (OM) with interactions based on just the double-folding model cannot reproduce the experimental data on elastic cross sections at near-barrier energies. A satisfactory description was achieved in the 80's with the development of a theoretical framework for performing coupled channel calculations, the coupled reaction channel calculations (CRC) and the continuum discretized coupled channel calculations (CDCC) [15, 16]. They can describe in a consistent manner the coupling to the breakup, neutron transfer, continuum states and the effect of the Coulomb dipole polarizability. These reaction channels can be included in an OM by the use of nuclear polarization potentials [17]. In the case of halo nuclei the nuclear potentials and parameterizations describing the scattering of stable nuclei cannot be just extrapolated and the role of the continuum and few-body correlations must be carefully taken into account [18]. These calculations are sensitive to structural parameters, like excited states and resonances, and the shape of the B(E1) distribution [10, 19]. New data becomes therefore important to test and extend this theoretical framework to the regions of most exotic nuclei (see [20] for a recent review).

## 2 PHYSICS CASE, OBJECTIVES AND PREDICTIONS

### *Physics case*

The neutron-rich carbon isotope $^{15}$C (t=2.45s) is weakly bound for one-neutron removal by only 1218 keV, and by 9395 keV for two-neutron removal [21, 22], suggesting the formation of a one-neutron halo structure. The spins and parities of the ground and first excited state (E= 740 keV) are known to be

$I^{\pi}=1/2^{+}$, $5/2^{+}$, respectively. These states are characterized by almost pure single-particle configurations where the $^{14}C$ core is coupled to an $s_{1/2}$ (ground) or $d_{5/2}$ (excited) orbital, with spectroscopic factors close to unity [23, 24]. In this respect $^{15}C$ would be a unique nuclear system in exhibiting a pure 2s1/2 single neutron halo ground state.

The halo structure of $^{15}C$ has been investigated at high energies in several experiments. The distribution of transverse-momentum for one-neutron breakup exhibits a width (FWHM) of 67(3) MeV/c, much smaller than its neighbour isotopes $^{14}C$ and $^{16}C$ (~ 200 MeV/c), although somehow larger than the typical value of ~ 40 MeV/c found for other well-known halo nuclei $^{11}Li$ or $^{6}He$ [2]. In [25] it was found that the reaction cross sections measured at 83 MeV/u showed an increase for the isotope $^{15}C$, which is absent at E=950 MeV/u. This behaviour could be attributed to the halo nature of $^{15}C$, where the couplings to breakup and transfer increase as the energy decreases. To investigate the influence of the neutron halo in the dynamics of the collision process it would be interesting to carry out scattering experiments at Colomb barrier energies, where these channels should play a dominant role.

Although it is potentially very interesting, there are no data related to elastic scattering of $^{15}C$ on medium to heavy nuclei at energies around the Coulomb barrier. However, coupled-channels calculations for elastic scattering of $^{15}C+^{208}Pb$ system at 54 MeV have been performed by Keeley and Alamanos [26]. They showed that the extended wave function of the valence neutron in 15C leads to a large transfer probability at large radii, larger than for more conventional nuclei. The inelastic channels and ($^{15}C$,$^{14}C$) transfer (Q=+2.70 MeV) were included, but not (15C,16C) (Q=−3.10 MeV) transfer. It was also suggested that breakup couplings might be as important as single-neutron transfer. Data on $^{15}C$ elastic scattering would be very welcome to check these possibilities [20].

### *Objectives*

We propose to study the scattering of $^{15}C$ with a $^{208}Pb$ target at $E_{Lab}$= 65 MeV ($E_{cm}$=60 MeV), just around the Coulomb barrier of this system. The main objective is to measure the angular distribution of the elastic cross section.

In principle we expect strong couplings between the elastic, neutron-transfer and direct breakup channels. The elastic data will be analyzed, in a first approach, by means of the optical model and polarization potentials to extract the relevant information. The explicit effects due to transfer and breakup mechanism can be described by the Coupled Channel calculations (CRC, CDCC). If properly tuned, the breakup process can be included in the optical potentials describing the entrance and exit channels in the CRC calculation, and the transfer process in the CDCC calculation, allowing for both calculations to reproduce in a consistent manner the measured angular distribution of the elastic scattering. This method should be appropriate when the coupling between breakup and transfer channels is weak, as we expect for the low energy scattering of $^{15}C$. This procedure was successfully used in the scattering of $^{6}He$ with $^{208}Pb$ [4-7]. Furthermore, the detector setup will obtain the angular and energy distributions of the $^{14}C$ fragments (Section 4), which can be used to further constrain the coupled channel calculations.

With the new data we will study relevant effects due to the halo structure of $^{15}C$: long-range absorption, dipole polarizability, consistency with B(E1) published values, OM potentials and comparison with systematics, and the coupling to neutron transfer, break-up channels and the continuum.

### *Predictions*

We have carried out coupled reaction channel calculations (CRC) describing the one-neutron stripping channel in system $^{15}C+^{208}Pb$ at 65 MeV. The $^{15}C$ halo has been modeled as a neutron plus an inert $^{14}C$ core, given that the first excited state of $^{14}C$ is high lying (> 6 MeV). The ground state was assumed to be a pure $^{14}C(0+)$ plus a neutron in the $2s_{1/2}$ level. Further details of this calculation can be found in [26].

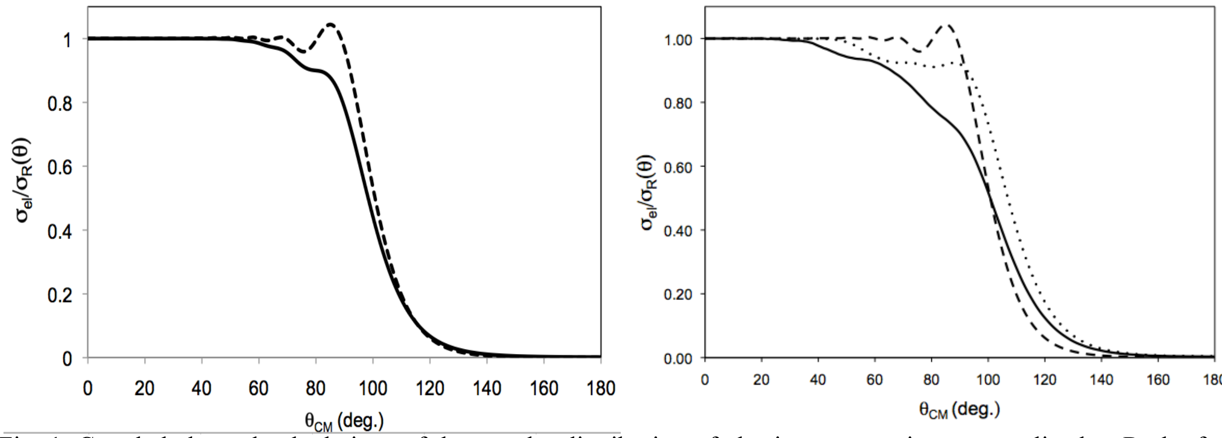


Fig. 1. Coupled channel calculations of the angular distribution of elastic cross sections, normalized to Rutherford, in the collision of $^{15}C$ + $^{208}Pb$ at 65 MeV. Left: Results of the CRC calculations including 1-n stripping. The solid line is the full calculation and the dashed line is obtained without coupling. Right: Results of the CDCC calculations including breakup and inelastic scattering. The solid line is the full calculation whereas the dashed line and the dotted line are obtained without couplings and with only nuclear couplings, respectively. See text for discussion.

In Fig. 1 (Left) we show the angular distribution of the elastic scattering, normalized to Rutherford, at E= 65 MeV. The dashed curve denotes the bare, no coupling, calculation and the solid one the result of the full calculation including the single-neutron stripping channel. We obtain a total reaction-cross section of 927 mb. The elastic cross-section shows a sizeable deviation from the bare calculation already above 60º, and a large reduction is observed around the grazing angle ~ 90º, a typical signature of the presence of a halo structure. The Coulomb rainbow has completely disappeared as expected for low energy scattering of a neutron halo system. However the most striking result is the large cross section obtained for the 1-n stripping channel (265 mb), and the strong effect on the angular distribution of the elastic scattering. We also find that the angular distribution of 1-n striping cross section exhibits a pronounced maximum (~70 mb/sr) in the angular region around 90º (not shown in the figure), and should be observed in the angular distribution of the $^{14}C$ yield.

The single neutron transfer alone would give a characteristic "strong coupling" shape to the elastic scattering angular distribution in this system. Similar effects were already found in the scattering of the two-neutron halo nuclei $^{6}He$ and $^{11}Li$ with $^{208}Pb$ at barrier energies. In the case of the one-neutron halo $^{15}C$, our calculations show that we should find a similar phenomenon by just considering the single neutron transfer channel. This large effect is due to the extended wave function of the valence neutron in $^{15}C$ (gs), which gives rise to a strong neutron transfer cross section already at large distances from the target. These results can be compared to that of stable $^{12,13}C$ scattering discussed in [26].

We have also carried out CDCC calculations to evaluate the contribution to the elastic scattering of the direct breakup channel and the transition to the 1st excited state (5/2+, 740 keV). The CDCC included the couplings to the bound, first excited state of $^{15}C$, as well as the L=0,1,2,3 of the n+$^{14}C$ continuum with couplings up to multipolarity $\lambda$ = 4. Further details of this calculation can be found in [27]. The CDCC calculation predicts a total reaction cross-section of 1379 mb, where the breakup contributes with 462 mb and the excitation to $^{15}C$ (5/2+, 740 keV) with only 45 mb. The angular distribution of the elastic cross-section, normalized to Rutherford, is shown in Fig. 1 (Right) with a solid line. The dashed curve denotes the calculation without couplings. This demonstrates the large effect on the elastic channel arising from the breakup channels, as expected for a halo nucleus. The dotted line is the result of a calculation including only the nuclear part of the coupling potentials. We find that not only the Coulomb, but also the nuclear couplings are important in the $^{15}C$ breakup, suggesting that it is closer in behaviour to $^{11}Be$ [8] than to $^{11}Li$ [9,10] or $^{6}He$ [4-7] where the Coulomb couplings were found to be dominant. The contribution of the inelastic scattering to ($5/2^{+}$, 740 keV) to the scattering process should be very small, below 10% of the reaction cross section according to our calculations. If the presence of this channel is more significant it can be extracted by our detector setup (Section 4).

By comparing the angular distribution of the elastic cross sections obtained by CRC and CDCC (solid lines in Fig 1) we can see that the effects on the elastic cross section due to breakup and 1-n stripping are quite different. If the breakup dominates the scattering process, we should observe a strong absorption in the elastic yield even at very forward angles, ranging from 10% to 40% between 40º to 90º degrees. This should also be reflected in the reaction cross sections, 50% larger in the case of breakup.

As a summary, we expect the elastic cross section of the system $^{15}C$ + $^{208}Pb$ at Coulomb barrier energies to be very sensitive to the coupling to the breakup and 1-n stripping channels, due to the halo structure of $^{15}C$.

## 3 EXPERIMENTAL OBSERVABLES TO BE MEASURED

The goal of this experiment is to measure the angular distribution of the elastic cross sections between 15º - 120º.

Nevertheless, the experiment can provide as well:

- The angular and energy distribution of $^{14}C$ yields. The 1-n stripping cross section estimated by CRC is about 30% of the reaction cross section, and should present a maximum around 90º. The CDCC predicts a breakup yield around 35% of the reaction cross section, which should concentrate at forward angles.
- Inelastic excitation of $^{15}C$. The CDCC calculations predict a small contribution, below 10% of reaction cross section, arising from the excitation of $^{15}C$ to the 5/2+ state at 740 keV. These events can be separated from the elastic channel by the energy difference, being much larger than our detector energy resolution (50 keV, typical).
- Fusion-evaporation. We have obtained for the fusion-evaporation cross section about 20% of the total reaction cross section, by using the code PACE4. The residual nuclei are short lived and will remain inside the reaction target. However, their alpha emissions, having decay energy in the energy range of 7-8 MeV, can be detected in our experimental setup.

## 4 EXPERIMENTAL SET-UP

The measurements will be carried out with the particle detector GLORIA [28], which was already used at GANIL (Caen, France) in the study of the $^{8}He$+$^{208}Pb$ system at Coulomb barrier energies [20, 29]. The detector array consists of six particle-telescopes arranged in a very close geometry around a rotated-target system, allowing for the measurement of reaction fragments in a continuous angular range from 15º to 165º (Lab). The total efficiency is 24% (geometrical).

By the use of two- stage DSSSD telescopes of 40 μm and 1 mm thickness, the detector array is able to resolve mass and charge of the elastic channel and the relevant reaction fragments. In Fig. 2 it is shown the results of a Monte Carlo simulation using light ions of Be, B, C in a range of detection energies between 20-80 MeV, at 21º Lab. The system can separate reaction events with one unit mass difference in the region of C isotopes with a figure-of-merit (FoM) close to unity. For a given isotope, the contribution arising from the relevant reaction channels can be disentangled by energy-angle correlations, as described in [28]. After the selection of a given isotope in the DE/E correlation plot, the events are further analyzed using the energy/angle correlation. A similar analysis can be carried out in the proposed experiment for $^{14}C$ events.

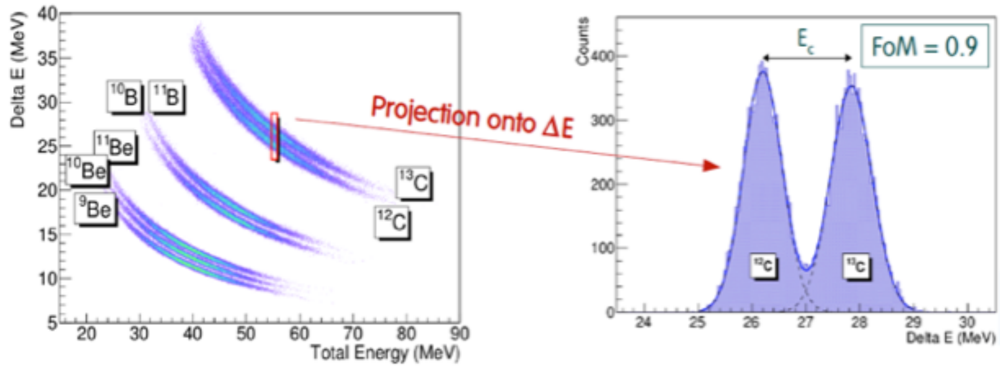


Fig. 2. Monte Carlo simulation of detector telescopes in GLORIA. Left: DE/E spectrum. Right: Mass separation between $^{12}C$ and $^{13}C$. See text for discussion.

## 5 BEAM REQUIREMENTS

We ask for 30 shifts on $^{15}C^{5+}$ with A/Q=3 at a beam energy of 65 MeV (4,3 MeV/u). This energy should be available during first phase at of HIE-ISOLDE after installation of the 2nd cryomodule [30].

The measured yield of $^{15}C$ is 7.9 x $10^5$ pps after the GPS, according to ISOLDE database. This value was obtained with a proton beam of 1.4 GeV and the CaO target. We estimate a rate of 4 x $10^4$ pps at reaction target assuming 5% efficiency in the transport and stripping process in EBIS. We estimated at 80º Lab a cross-section of 450 mb/sr for the elastic channel and 50 mb/sr for the single-neutron stripping channel. The detector GLORIA provides a solid angle of 50 msr for each observation angle with 3 degrees angular width. With a $^{208}Pb$ target of 1,3 mg/cm$^2$ thickness we expect a count rate of 12 counts per hour for the elastic channel and 1,5 counts per hour for the single-neutron stripping channel. With the requested 30 shifts we can achieve a total statistical error in the angular distributions of elastic and transfer channels around 4% and 10%, respectively. This is sufficient to observe the effects predicted by the coupled channel calculations.

Having the same A/Q ratio as $^{15}C^{5+}$, we expect the presence of $^{15}N^{5+}$ at 65 MeV as a possible beam contaminant. Previous measurements give an intensity of about 4 x $10^6$ pps on target. However the Coulomb Barrier for $^{15}N$ + $^{208}Pb$ system is around 76 MeV, and a pure Rutherford scattering is expected. In the telescope mass spectrum, the $^{15}N$ events will lie above the carbon region shown in Fig. 4, and will be separated and analyzed. This data will be useful for normalizing our scattering cross sections and to reduce uncertainties in the scattering angles and solid angle calculations.

We have however considered the possibility of reducing the fraction of $^{15}N/^{15}C$ carbon ions to avoid possible dead-time problems in our data acquisition system. We can extract the beam of $^{15}C^{5+}$ from EBIS and then use stripper foils to select $^{15}C^{6+}$. The estimated suppression factor for $^{15}N^{5+}$ is estimated around ~100 at 4.3 MeV/u, and the stripping efficiency to pass from $5^+$ to $6^+$ in C is close to 100%. Using this configuration a rate of about 4x$10^4$ $^{15}N^{5+}$ pps will be transmitted to the experiment. We can further reduce the yield of $^{15}N$ by using TOF between the arrival of the proton pulse and the events detected at GLORIA.

The radiation levels from the beam and the decay of it (as well as any reaction-induced activity) will be sufficiently low to not cause any problems. The Si detectors for charged particle identification do not pose any safety risks.

**Summary of requested shifts:**

We ask for 30 shifts of $^{15}C$ at 65 MeV. Average beam intensity 4 x $10^4$ pps on the secondary target.

**Beamline:** 2nd beamline at HIE-ISOLDE.

**References**


[1] I. Tanihata et al., Phys. Rev. Lett., 55 (1985) 2676; P.G. Hansen and B. Johnson, Europhys. Lett 4 (1987) 409.
[2] T. Aumann, Eur. Phys. J. A 26, (2005) 441.
[3] N. Keeley, et al., Phys Rev. C 88 (2013) 017602.
[4] L. Standylo et al., Phys. Rev. C 87 (2013)064603.
[5] K. Rusek et al, Acta Phys. Pol B 43 (2012) 233-238.
[6] D. Escrig et. al., Nucl. Phys. A 792 (2007) 02.
[7] A. M. Sánchez-Benítez et al., Nucl. Phys. A 803 (2008) 30.
[8] L. Acosta et al., Phys. Rev. C 84 (2012) 044604.
[9] M. Cubero et al., Phys. Rev. Lett. 109 (2012) 262701.
[10] J. P. Fernández-García et al., Phys. Rev. Lett. 110 (2013) 142701, Phys. Rev. C 92 (2015)014604.
[11] E.F. Aguilera et al., Phys. Rev. C 81, 011604(R) (2010); Phys. Rev. Lett. 88 (2000) 5058; Phys. Rev. C 63 (2001) 061063 (R).
[12] I. Martel, AIP Conf. Proc. 1423 (2011) 89.
[13]. Liu Zu-Hua, Chin.Phys.Lett 21(2004)40
[14] N. C. Summers and F. M. Nunes, Phys. Rev. C 78, 011601(R) (2008)
[15] G.R. Satchler, Direct Nuclear Reactions, Oxford Univ. Press, New York, 1983.
[16] A. Deltuva et al., Phys. Rev. C 76, 064602 (2007)
[17] K. Rusek et al., Phys. Rev. C 72, 037603 (2005)
[18] M. Rodríguez-Gallardo et al. Phys. Rev. C 77 (2008) 064609. V. Morcelle et al., Phys. Lett. B 732 (2014) 228; W. S. Hwash et al, Int. J. Mod. Phys. E 21, 1250066 (2012); M.V. Zhukov et al., Phys. Rep. 211(1993) 151.
[19] V. Parkar et al., Acta Phys. Pol. B 42 (2011) 3.
[20] J.J. Kolata et al., Eur. Phys. J. A (2016) 52: 123
[21] F. Ajzenberg-Selove, Nucl. Phys. A523 (1991) 1.
[22] G. Murillo, S. Sen, S.E. Darden, Nucl. Phys. A 579 (1994) 125.
[23] J.R. Terry, et al., Phys. Rev. C 69 (2004) 054306.
[24] S. Truong, Phys. Rev. C 28 (1983) 977.
[25] A. Ozawa, Nucl. Phys. A738 (2004) 3844.
[26] N. Keeley, K.W. Kemper and K. Rusek, Eur. Phys. J. A 50 (2014) 145.
[27] N. Keeley and N. Alamanos, Phys. Rev. C 75 (2007) 054610.
[28] G. Marquínez-Durán, Nucl. Inst. Meth. A755 (2014) 69.
[29] G. Marquínez-Durán et al., Acta Phys. Pol. B 47 (2016).
[30] A. Herlert and Y. Kadi , "The HIE-ISOLDE Project" Journal of Physics: Conference Series 312 (2011) 052010.

**Appendix**

## DESCRIPTION OF THE PROPOSED EXPERIMENT

The experimental setup comprises: *(name the fixed-ISOLDE installations, as well as flexible elements of the experiment)*

| Part of the Choose an item. | Availability | Design and manufacturing |
|---|---|---|
| Silicon detector system GLORIA [*] | ☒ Existing | ☒ To be used without any modification<br>☐ To be modified |
| General purpose Reaction Chamber at HIE-ISOLDE line 2. | ☒ Existing | ☒ To be used without any modification<br>☐ To be modified |

* G. Marquinez-Duran, et al. "GLORIA: A compact detector system for studying heavy ion reactions using radioactive beams". Nuclear Instruments & Methods in Physics Research Section A 755 (2014) 69-77.

## HAZARDS GENERATED BY THE EXPERIMENT

*(if using fixed installation)* Hazards named in the document relevant for the fixed [MINIBALL + only CD, MINIBALL + T-REX] installation.

Additional hazards:

| ***Hazards*** | | | |
|---|---|---|---|
| | *[Part 1 of the experiment/equipment]* | *[Part 2 of the experiment/equipment]* | *[Part 3 of the experiment/equipment]* |
| Thermodynamic and fluidic | | | |
| Pressure | | | |
| Vacuum | $10^{-6}$ mb | | |
| Temperature | Room temperature | | |
| Heat transfer | | | |
| Thermal properties of materials | | | |
| Cryogenic fluid | | | |
| Electrical and electromagnetic | | | |
| Electricity | | | |
| Static electricity | | | |
| Magnetic field | | | |
| Batteries | | | |
| Capacitors | | | |
| Ionizing radiation | | | |
| Target material | Primary:<br>CaO | Secondary:<br>$^{208}$Pb, 1.3 mg/cm$^2$ | |
| Beam particle type | Primary: | Secondary: | |

| | | | |
|---|---|---|---|
| (e, p, ions, etc) | p | $^{15}C$ | |
| Beam intensity | Primary beam:<br>p, at primary target<br>$3.10^{13}$ per pulse (2 ms) | Secondary beam:<br>$^{15}C$, secondary target<br>$7.9 \times 10^5$ pps | |
| Beam energy | Primary beam:<br>p, at primary target,<br>1.4 GeV | Secondary beam:<br>$^{15}C$, secondary target<br>4.3 MeV/u | |
| Cooling liquids | | | |
| Gases | | | |
| Calibration sources: | | | |
| • Open source | X | | |
| • Sealed source | | | |
| • Isotope | $^{241}Am$ | | |
| • Activity | 300 kBq (alpha) | | |
| Use of activated material: | NO | | |
| • Description | | | |
| • Dose rate on contact and in 10 cm distance | | | |
| • Isotope | | | |
| • Activity | | | |
| Non-ionizing radiation | | | |
| Laser | | | |
| UV light | | | |
| Microwaves (300MHz-30 GHz) | | | |
| Radiofrequency (1-300MHz) | | | |
| | | | |
| Toxic | | | |
| Harmful | | | |
| CMR (carcinogens, mutagens and substances toxic to reproduction) | | | |
| Corrosive | | | |
| Irritant | | | |
| Flammable | | | |
| Oxidizing | | | |
| Explosiveness | | | |
| Asphyxiant | | | |
| Dangerous for the environment | | | |
| | | | |
| Physical impact or mechanical energy (moving parts) | | | |

| | | | |
|---|---|---|---|
| Mechanical properties (Sharp, rough, slippery) | | | |
| Vibration | | | |
| Vehicles and Means of Transport | | | |
| | | | |
| Frequency | | | |
| Intensity | | | |
| Physical | | | |
| Confined spaces | Bat.170, 1 Rack for electronics and dacq | | |
| High workplaces | | | |
| Access to high workplaces | | | |
| Obstructions in passageways | | | |
| Manual handling | | | |
| Poor ergonomics | | | |

### 0.1 Hazard identification

3.2 Average electrical power requirements (excluding fixed ISOLDE-installation mentioned above): *(make a rough estimate of the total power consumption of the additional equipment used in the experiment: 20 kW*